Welding in the World (2019) 63:913–924
https://doi.org/10.1007/s40194-019-00720-5

RESEARCH PAPER

Experimental and numerical modeling study of solidification cracking in Alloy 52M filler metal in the cast pin tear test

Huimin Wang[1,2] · Boian T. Alexandrov[2] · Eric Przybylowicz[2,3]

Received: 17 December 2018 / Accepted: 22 February 2019 / Published online: 4 March 2019
© International Institute of Welding 2019

Abstract

Finite element analysis (FEA) model of the solidification process in the cast pin tear test (CPTT) was developed using the commercial software ProCAST™. Modeling predictions of the solidification and strain accumulation sequences and of the cracking sensitive region location were validated using parallel CPTT testing of Alloy 52M filler metal. Predicted pin length dependences of the hot tearing indicator (HTI) and the effective plastic strain (EPS) were in good correlation with the experimentally determined zero to 100% CPTT cracking curve in Alloy 52 M. Sensitivity study with the developed model identified material properties and test parameters with strong influence on the accuracy of modeling predictions. Parallel computational modeling and CPTT experimentation was performed to quantify the critical strain for solidification cracking in Alloy 52M filler metal. This study demonstrated that numerical modeling of weldability tests can be used for quantification of material-specific properties related to cracking susceptibility in engineering alloys.

Keywords Numerical modeling · Cast pin tear test · Solidification cracking · Hot tearing indicator · Critical strain · Alloy 52M

1 Introduction

Primary water stress corrosion cracking (PWSCC) in dissimilar metal welds (stainless steel to low alloy steel) is a common issue in the primary contour of nuclear power plants [1]. Structural welds overlays (SWOLs) have been used to mitigate PWSCC for decades [2–4]. The SWLOs were developed as a repair method to provide a pressure boundary and introduce compressive stresses that would prevent propagation of SCC [5]. Alloy 52M filler metal demonstrated high resistance to SCC and was introduced as a replacement of Alloy 600, originally used in SWOLs [6, 7]. The high Cr content in Alloy 52M prevents Cr depletion at the grain boundaries. Coherent $Cr_{23}C_6$ intergranular carbides have significant effect on inhibiting PWSCC [7]. However, in some cases, solidification cracking occurred in SWOLs of Alloy 52M on cast stainless steel pipe substrate [8] due to dilution of iron from the stainless steel in the weld pool [2]. High iron content increases niobium partitioning, which causes widening of the solidification temperature range by forming a low-melting eutectic constituent containing NbC [2]. Wider solidification ranges can promote accumulation of plastic strain in the mushy zone that is sufficient to cause cracking at the terminal stage of solidification. A combination of experimental and computational methods was used in this study, aiming to quantify the critical plastic strain accumulation for solidification cracking in Alloy 52M filler metal within the cast pin tear test (CPTT).

The CPTT is used as a tool for evaluation of the susceptibility to solidification cracking in metallic alloys. It was originally developed by F.C. Hull in the 1960s to rank the susceptibility to hot cracking in stainless steel during welding and casting [9]. Recently, CPTT has been modified at The Ohio State University to study the solidification cracking susceptibility in high chromium nickel-base welding filler metals

Recommended for publication by Commission IX - Behaviour of Metals Subjected to Welding

✉ Huimin Wang
wanghuimin@ustb.edu.cn

✉ Boian T. Alexandrov
alexandrov.1@osu.edu

[1] National Center for Materials Service Safety, University of Science and Technology Beijing, 30 Xueyuan Rd, Haidian District, Beijing 100083, China

[2] Welding Engineering Program, Department of Materials Science and Engineering, The Ohio State University, 1248 Arthur E. Adams Dr, Columbus, OH 43221, USA

[3] Honeywell Aerospace, Tempe, AZ, USA

[10–12]. The CPTT is a self-restraint test, in which the strain applied to the test sample (cast pin) is caused by solidification and solid-state shrinkage of the pin, and thermal expansion of the mold. The strain applied to the last solidifying portion of the cast pin increases with the pin length [9]. The CPTT ranks susceptibility to solidification cracking by utilizing the maximum pin length without cracking and the minimum pin length with 100% cracking as the ranking criteria. Rankings of susceptibility to solidification cracking in several high chromium nickel-based alloys generated using CPTT were consistent with Transvarestraint test results [10, 12–14].

Significant advantages of the CPTT in comparison to other solidification cracking tests include the small amount of material needed for testing and the ability to evaluate the effect of dilution on solidification cracking susceptibility in dissimilar metal combinations. However, the local strain that causes cracking in the CPTT, as well as in the other available solidification cracking tests, is difficult to measure experimentally. A potential solution of this problem is the development of computational models for such tests that can be used to study the cracking behavior and quantify the critical strain for solidification cracking.

Computational modeling using finite element analysis (FEA) has been extensively applied to relate the chemistry, heat transfer, fluid flow [15], etc. to the microstructure [16] and defect formation in welded joints [17, 18]. Solidification cracking is one of the common defects related to the chemical composition, solidification morphology, and thermal and mechanical loads experienced in welds [19]. Several solidification cracking models have been developed. According to the strain-driven model, solidification cracking occurs when the strain accumulated during solidification exceeds the ductility of the material in the mushy zone [20]. Safari et al. studied the solidification cracking of stainless steel 310s with a commercial software, ABAQUS™ [20]. They identified that the maximum transverse strain determined the propagation of solidification cracks. The strain rate–driven model assumes that solidification cracking occurs when the strain rate or strain rate–related pressure reaches a limit [16]. Neil et al. studied the hot cracking in aluminum alloy 6061 utilizing the theory developed by Rappaz, Drezet, and Gremaud (RDG) [16]. The strain rate–related pressure along the columnar grains was calculated to predict the onset of solidification cracking in 6061 aluminum. The predicted location of cracking onset was consistent with in situ observations. The stress-driven model is based on the assumption that solidification cracking occurs when the stress exceeds a critical value [21] in the mushy zone.

In the commercial software ProCAST™, a module named hot tearing indicator (HTI) considers the evolution of strain, stress, and strain rate at the last stage of solidification [22]. This is expressed in Eq. 1, where e_{ht} is the hot tear indicator, t_{c} is the coherency temperature, t_{s} is the solidus temperature, and ε^{p} is plastic strain. The HTI represents the accumulation of the plastic strain in the mushy zone. This model has been validated by experimental study on solidification of a Mg-Al alloy. In the study of yttrium effect on the solidification cracking of Mg-Y alloy, the predicated hot tearing susceptibility agreed with the experimental measurements [23].

$$e_{ht} = \int_{t_c}^{t} \sqrt{(2/3)\dot{\varepsilon}^{p} : \dot{\varepsilon}^{p}}\, d\tau, (t_c \le \tau \le t_s) \tag{1}$$

Simulations with ProCAST™ were previously used in the development of the new generation CPTT, aiming to optimize the mold design for better replication of weld cooling rates, predict solidification sequences, and determine interfacial heat transfer coefficients [12, 24].

The objective of this study was to demonstrate the approach for computational modeling of weldability tests as a tool for quantification of material-specific properties related to cracking susceptibility. Such properties, i.e., the critical plastic strain accumulation for solidification cracking, can be used as a reference in the design of welded components and development of welding procedures. Computational modeling of the CPTT using ProCast™ and testing with the new generation CPTT were utilized to quantify the critical strain for solidification cracking in Alloy 52M filler metal. The solidification behavior of Alloy 52M was also predicted and compared with experimental results, including the location of cracking sensitive region and direction of crack propagation.

2 Materials and procedures

The chemical compositions of Alloy of 52M filler metal and Al-bronze C63000 mold material used in this study are shown in Table 1. C63000 was selected as the mold material since it was found to provide cooling rates, within the solidification temperature range of Ni-based alloys, that are comparable to conventional GTAW [12].

Table 1 Chemical composition of Alloy 52M and C63000 (wt%)

Alloy	Al	Sn	Zn	Cu	C	Cr	Fe	Mn	Mo	Nb	Ni	P	S	Si	Ti
52 M	0.12	–	–	0.03	0.017	30.01	8.51	0.72	0.01	0.81	59.41	0.003	0.001	0.12	0.21
C63000	9.0–11.0	0.2	0.3	balance	–	–	2.0–4.0	1.5	–	–	4.0–5.5	–	–	0.25	–

Table 2 Mass of Alloy 52M buttons required for different mold lengths

Length (in)	0.75	0.875	1	1.125	1.25	1.375	1.5	1.625	1.75	1.875	2	2.125	2.25	2.375	2.5
Mass (g)	10.5	11	11.5	12	12.5	13	13.5	14	14.5	15	15.5	16	16.5	17	17.5

The solidification cracking susceptibility of Alloy 52 filler metal was tested using the new generation CPTT device developed by Luskin et al. [12, 25]. The latter utilizes induction levitation melting with microprocessor control of all test parameters, including induction current ramp and down slope, casting temperature, shielding gas pressure, and flow rate.

The Alloy 52M filler metal was cleaned with alcohol and melt in buttons with weights corresponding to mold/cast pin lengths between 0.75 in. and 2.5 in. (Table 2) [13]. The buttons were prepared using gas-tungsten arc torch over a cooled copper hearth in an argon-purged chamber. The testing was performed with the new generation CPTT following the detailed procedures described in [12]. Three to five pins were cast at each mold length. Crack lengths on the cast pin surface were measured in degrees using a binocular microscope. The circumferential cracking was calculated using Eq. 2, where L_T is the total length of all cracks measured on the pin surface.

$$Circumferential\_cracking(\%) = \frac{L_T^0}{360^0} \times 100\% \quad (2)$$

3 FEA model of the cast pin tear test

A 3D model of the CPTT was built with Solidworks™ and used with the ProCAST™ software in FEA modeling of the solidification behavior and quantification of the hot tear indicator and the local strain accumulation in cast pins of Alloy 52M. The 3D FEA model included the cylindrical mold, the bottom disk, and the cast pin. The cast pin diameter was 5 mm (0.197 in.) and the pin length was defined as the cylindrical portion between the pin head and foot. In this study, cast pins with lengths of 0.5 in., 1.0 in., 1.5 in., 2.0 in., and 2.5 in. were numerically simulated. During solidification, the pin acts as a tensile test sample due to the shrinkage of the pin and expansion of the mold. The tensile strain generated during solidification accumulates in the last solidified portion of the pin.

The following materials were assigned to the FEA model in ProCAST™: Alloy 52M for the cast pin, Al-bronze C63000 for the mold, and technically pure copper C1100 for the bottom disk. The FEA model was meshed in ProCAST™ using 3D solid tetrahedral elements with size of 0.5 mm as shown in Fig. 1.

Elasto-plastic behavior was assigned to the cast pin (Alloy 52M), while the C63000 mold was assumed as rigid. The thermophysical and thermomechanical properties Alloy 52M were calculated using the commercial software JMatPro™. A plot of the temperature-dependent density, thermal conductivity, Young's modulus, and Poisson's ratio of Alloy 52M is shown in Fig. 2. The non-equilibrium solidus and liquidus temperatures of

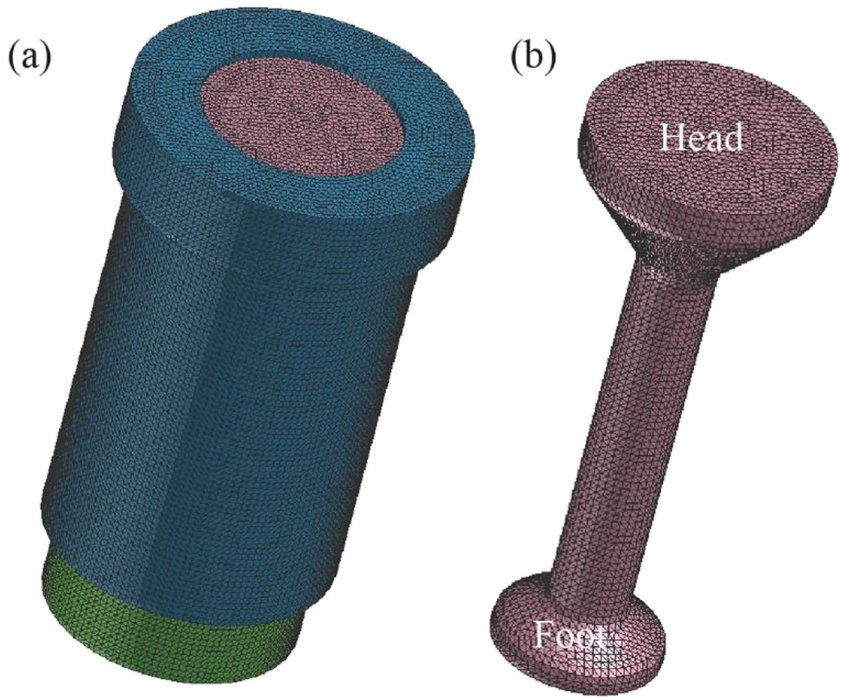

Fig. 1 **a** Meshed 3D model of the Alloy C3600 mold and pin. **b** Meshed 3D model of Alloy 52M cast pin

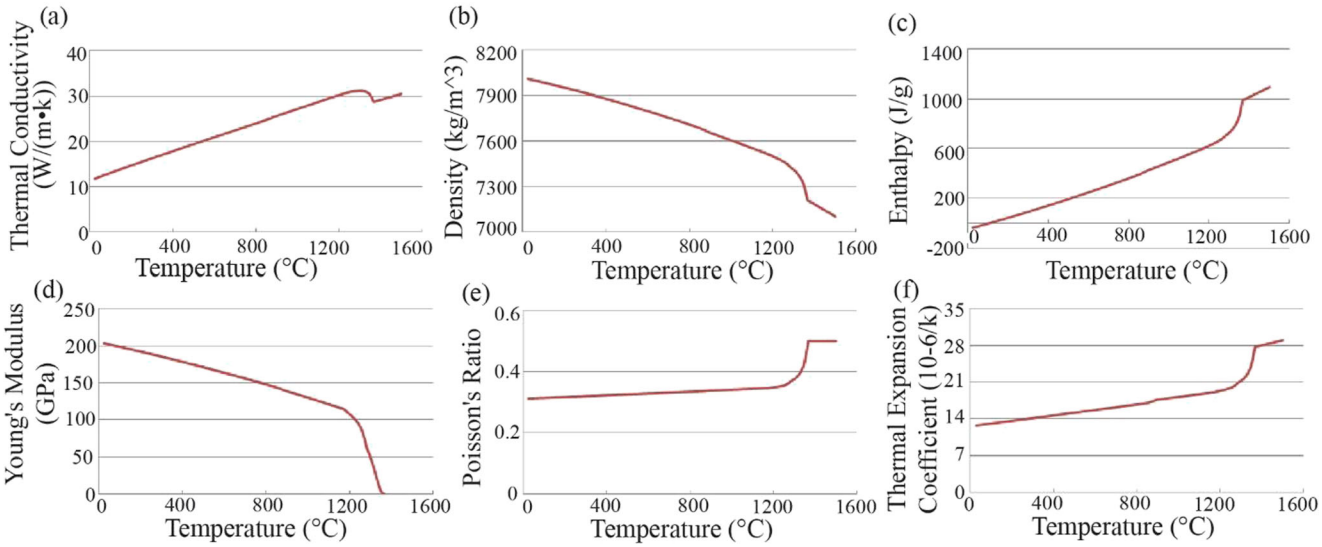

Fig. 2 Thermophysical and thermomechanical properties of Alloy 52M predicted with JMatPro™

Alloy 52M were predicted using the Scheil-Gulliver module of ThemoCalc™ as 1210 °C and 1366 °C correspondingly. The predicted solidification range of 156 °C was close to SS DTA measured value for Alloy 52M [10, 14]. The temperature dependence of the interfacial heat transfer coefficient between the cast pin and the mold was determined using the inverse modeling module of ProCAST™ (Fig. 3) [12]. The latter is based on optimization of the interfacial heat transfer coefficient to achieve closest match of a predicted cooling rate to actually measured one.

The boundary condition at the external mold surface was set as air cooling with initial temperature of 20 °C. The alloy was poured into the mold by gravity (9.8 m/s^2) with an initial temperature of 1500 °C. The filling time for a 2.0-in. long pin was estimated from experimentation as 0.1 s. A filling rate 0.15699 Kg/s was calculated and applied for all tested pin lengths.

4 Results and discussion

4.1 Solidification cracking susceptibility in Alloy 52M filler metal

The CPTT results for Alloy 52M are plotted in Fig. 4. Pins with no cracking and pins with occasional crack initiation of less than 5% surface cracking were identified at 0.75 in. and 0.875 in. pin lengths. The minimum pin length with consistent crack initiation and the minimum pin length with consistent full separation (100% cracking) were correspondingly 1.0 in. and 2.0 in. There was a gradual increase in the percentage of circumferential cracking between the 0.875 in. and 2.0 in. pin lengths with wider variation in the cracking extent at longer pins. The fracture surfaces in failed cast pins exhibited a typical solidification cracking morphology with exposed dendrites and presence of low-melting point eutectic constituent within the interdendritic spaces (Fig. 5 (a)). Cracking usually

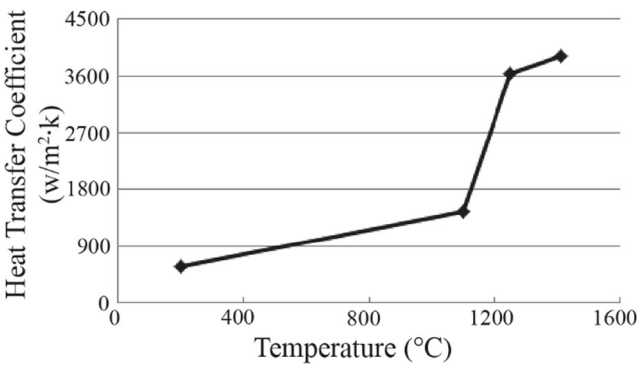

Fig. 3 Interfacial heat transfer coefficient between cast pin of Alloy 52M and Alloy C63000 mold

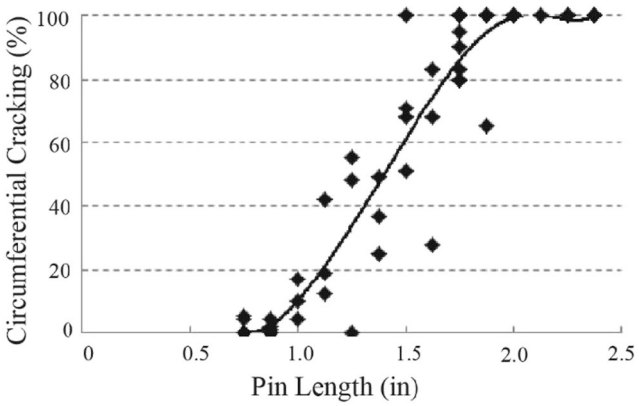

Fig. 4 Experimentally determined percentage circumferential cracking in cast pins of Alloy 52M

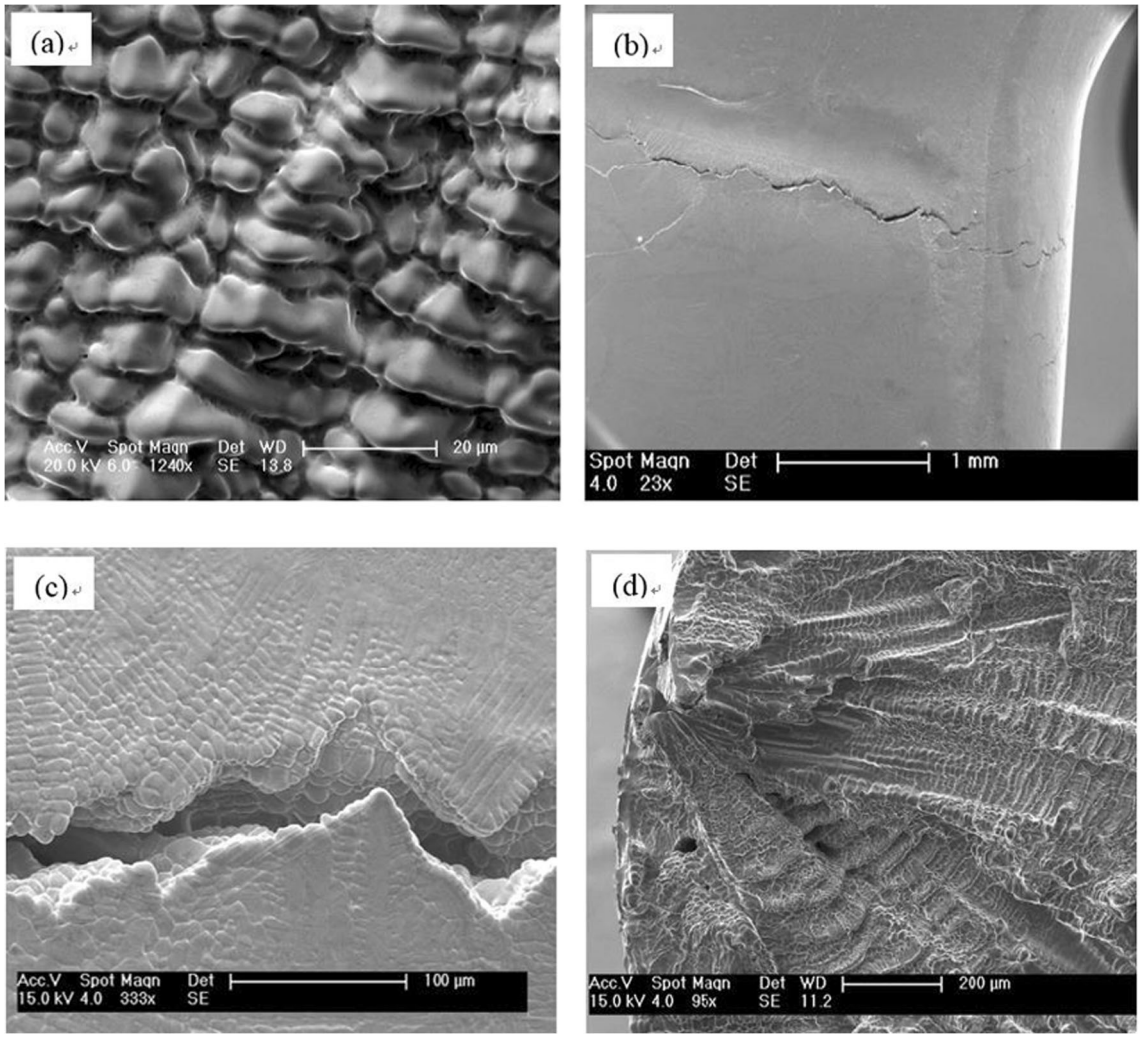

Fig. 5 Solidification cracking in cast pins of Alloy 52M: **a** fracture surface morphology of 2.0-in. long cast pin with full separation (100% cracking), **b** typical crack location in CPTT pins, **c** surface crack initiation 1.5-in. long cast pin with 53% circumferential cracking, **d** surface crack initiation in fully separated 2.5-in. long cast pin

occurred in the pin neck area just beneath the pin head (Fig. 5 (b)). Examples of crack nucleation at the pin surface and propagation towards the pin centerline, which is the typical fracture sequence in the CPTT, are shown in Fig. 5 (c) and (d).

4.2 Solidification sequence and plastic strain accumulation

The developed FEA model of CPTT in the ProCast™ software was used to simulate the solidification sequences and plastic strain generation in a series of Alloy 52M cast pins. The effective plastic strain (EPS) parameter calculated by the ProCAST™ was utilized in this study. A particular solution for a 2.0-in. long pin is shown in Fig. 6. The contour plots of fraction solid show that solidification starts from the mold/liquid contact interface and progresses towards the pin center line. Metallurgical characterization with light optical microscopy and scanning electron microscopy revealed a typical columnar dendritic solidification with nucleation off the mold surface and growth towards the pin centerline [12]. Therefore, the FEA prediction is consistent with the experimentally observed solidification morphology. Since the pin head is acting as a large reservoir of liquid and a heat source, the pin neck and head are predicted to solidify last. Similar solidification behavior in cast pins of Alloy 52M at faster heat extraction conditions (Cu-Be mold of different geometry) was predicted by Luskin et al. [12].

Along with the formation of a solid layer at the mold surface, strain accumulation begins from the pin surface following the solidification sequences towards the pin centerline. As shown in Fig. 6, the gradient in EPS is related to the fraction solid. Local EPS concentration in the range of 1% occurs at the surface of the pin neck, which is predicted to solidify last. The predicted location of strain concentration and direction of strain accumulation in cast pins of Alloy 52M fully coincide with the typical crack nucleation

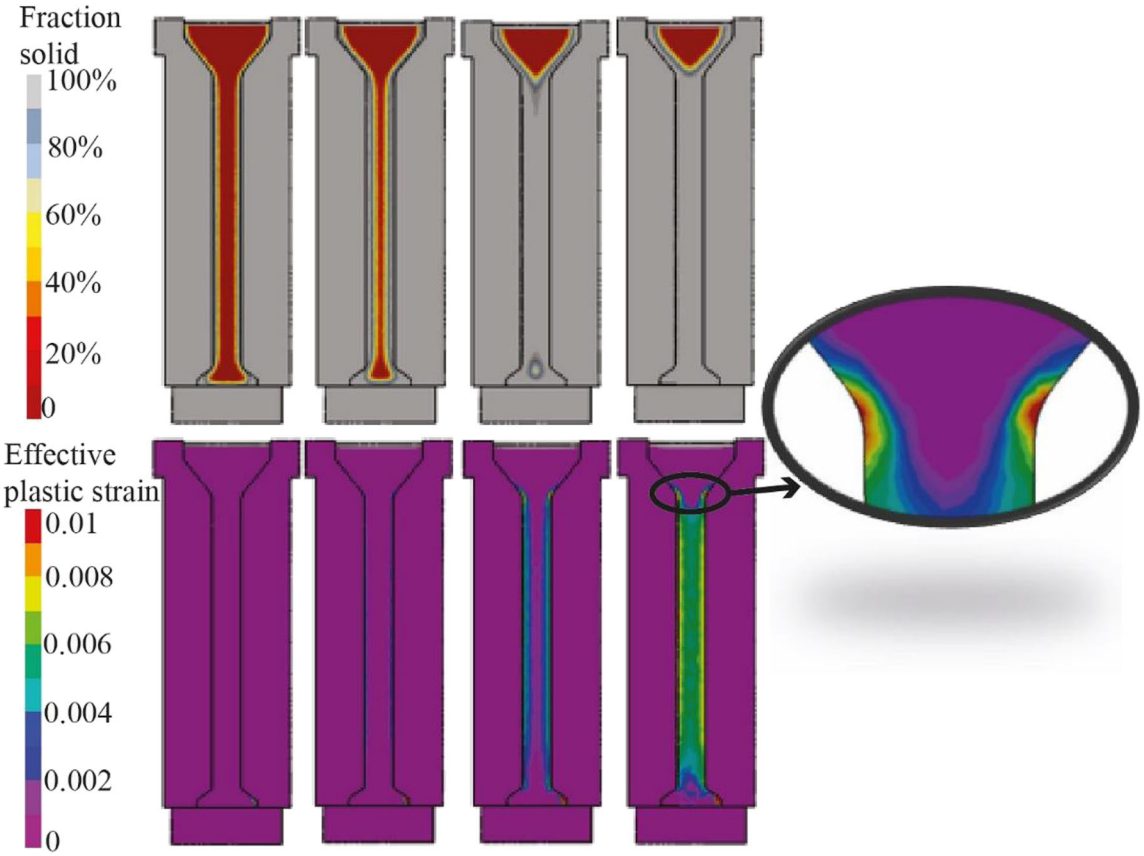

Fig. 6 Predicted sequence of solidification and plastic strain accumulation in a 2.0-in. long cast pin of Alloy 52M

site and direction of crack propagation in the actual CPTT experiments shown in Fig. 5.

4.3 Hot tearing indicator and circumferential cracking

Predicted HTI distribution contours at the surfaces and cross sections of the five pin lengths subjected to FEA simulations are displayed in Fig. 7. For each pin length, the maximum value of the HTI appeared in the pin neck region (beneath the pin head). The HTI exhibited a strong decreasing gradient, in the cast pin cross section, from the pin surface towards the pin centerline. These predictions correlate with the predicted EPS distribution and solidification sequence shown in Fig. 6, and indicate that solidification cracking would initiate at the pin surface and would propagate towards the pin centerline. Therefore, the predicted solidification cracking sensitive region in cast pins of Alloy 52M is located at the pin surface and cross-section just beneath the pin head. These modeling predictions fully coincide with the experimental observations of the crack sensitive region, crack initiation, and crack propagation in cast pins of Alloy 52M shown in Fig. 5.

The average HTI for the cracking sensitive regions (the region highlighted in Fig. 10, surface values were used) of all simulated pins was calculated and plotted versus the pin length as shown in Fig. 8. The average HTI increased gradually between 0.5 in. and 1.5 in. pin lengths and almost leveled at 2.0 in. pin length. This trend correlated with the experimentally determined gradual increase in percentage of circumferential cracking between the maximum pin length with no cracking (0.857 in.) and the minimum pin length with 100% cracking (2.0 in.) shown in Fig. 4. HTI value of 0.014 corresponded to the experimentally determined minimum pin length of 1.0 in. at which consistent cracking occurred in the tested alloy. This can be considered as the critical HTI value for initiation of solidification cracking in Alloy 52M.

4.4 Critical strain for solidification cracking of Alloy 52M in the CPTT

The effective plastic strain (EPS) in the cracking sensitive region was predicted for pin lengths between 0.5 in. and 2.0 in. These pin lengths corresponded to the ranges of zero to 100% circumferential cracking and of gradual increase in the HTI shown in Figs. 4 and 8. The average EPS within the crack sensitive region of all simulated pin lengths was plotted versus the fraction solid in Fig. 9. For all pin lengths, the average EPS value was close to zero below 0.88 fraction solid and gradually increased to about 0.5% as the fraction solid increased to 0.97. Above that point, the EPS behavior was similar for all pin lengths: gradual increase to a plateau

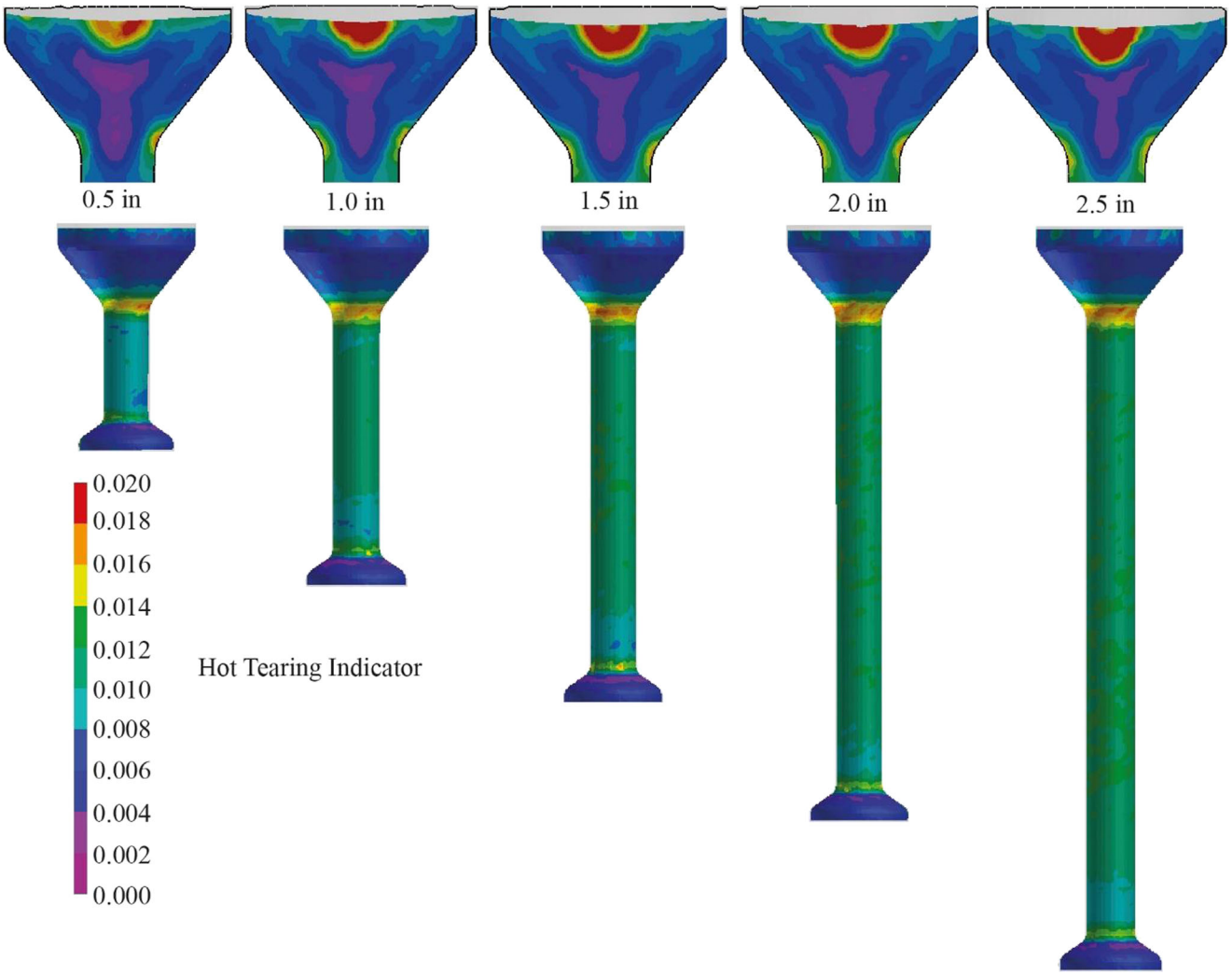

Fig. 7 FEA predicted HTI contours at the surface and cross sections of cast pins in Alloy 52M

followed by a sharp rise at the end of solidification. The EPS values characterizing the strain accumulation within the cracking sensitive region during the final stage of the solidification process are summarized in Table 3.

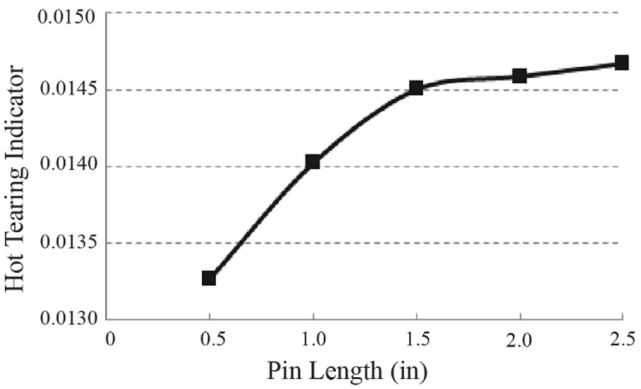

Fig. 8 FEA predicted average HTI for the cracking sensitive region of cast pins in Alloy 52M

With increasing the pin length from 0.5 to 1.0 and 1.5 in., the EPS plateaus occurred at lower fraction solid. Longer pins experienced larger EPS values, both at the EPS plateaus and at the end of the solidification process (at 0.999 and 1.0 fraction solid). The 1.5 and 2.0 in. pins had similar EPS values above 0.97 fraction solid, with the former reaching slightly higher EPS values within the plateau.

The critical strain for solidification cracking in Alloy 52M can be estimated by comparing the predicted EPS dependence on fraction solid (Fig. 9), to the CPTT generated circumferential cracking dependence on pin length (Fig. 4). Since the 0.75 in. and 0.875 in. pin lengths exhibited occasional surface crack initiation in the CPTT (Fig. 4), for the purpose of this study, pin length of 0.5 in. can be considered as a the maximum pin length with no cracking. Therefore, the predicted EPS value of 0.747% at the end of solidification process in the 0.5 in. pin, corresponding to 0.999 solid fraction, can be considered as the maximum level of local strain accumulation that Alloy 52M would sustain without solidification cracking.

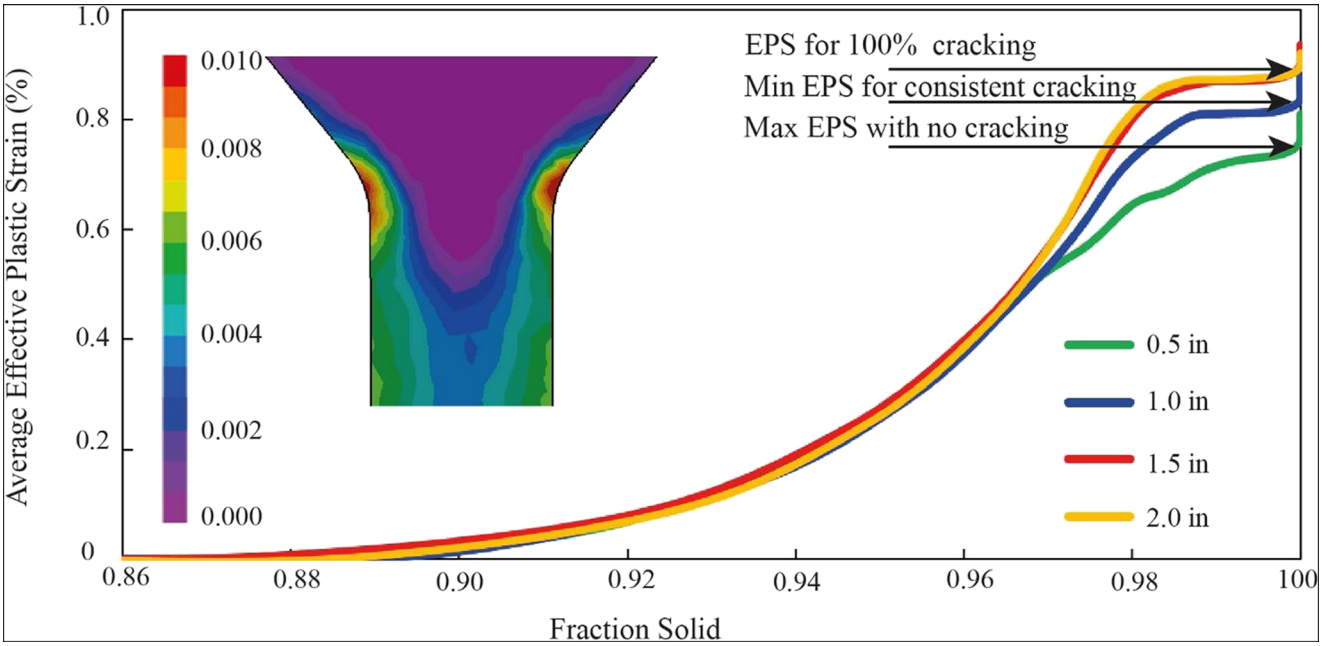

Fig. 9 Average effective plastic strain in the cracking sensitive region of cast pins in Alloy 52M. The EPS contour shows region of strain concentration in the cracking sensitive region beneath the pin head

Similarly, the predicted EPS value of 0.825% at the end of solidification in the 1.0 in. pin, which was the minimum pin length with consistent cracking, can be assumed as the lowest strain that would consistently cause solidification cracking in cast pin tear testing of Alloy 52M.

Based on the results of this study, the predicted critical EPS range for solidification cracking in CPTT of Alloy 52M can be defined as 0.75 to 0.83%. For the 1-in. long pin, this strain range corresponded to a predicted solid faction ranges between 0.981 and 0.999. The predicted strain for consistent 100% cracking in the 2.0 in. pin can be estimated as 0.88% at 0.999 fraction solid. The 1.5 in. pin length exhibited variable cracking response between 51% and 100% circumferential cracking that corresponded to a predicted EPS range from 0.83 to 0.88%.

Such narrow range of the predicted EPS, from consistent crack initiation through 100% cracking, could provide an explanation for variations in the CPTT percentage cracking at pin lengths above the crack initiation threshold. Previous experience with the CPTT has shown very good resolution in determining the cracking threshold (maximum pin length with no cracking) and larger result variations in the range between no cracking and consistent 100% cracking. A specially designed investigation with the developed FEA model in ProCAST™ can be performed to improve the reproducibility of CPTT results throughout the whole cracking range by further optimization of the CPTT mold design.

The predicted critical ranges of local strain accumulation and fraction solid for solidification cracking in Alloy 52M are in good correspondence with experimental

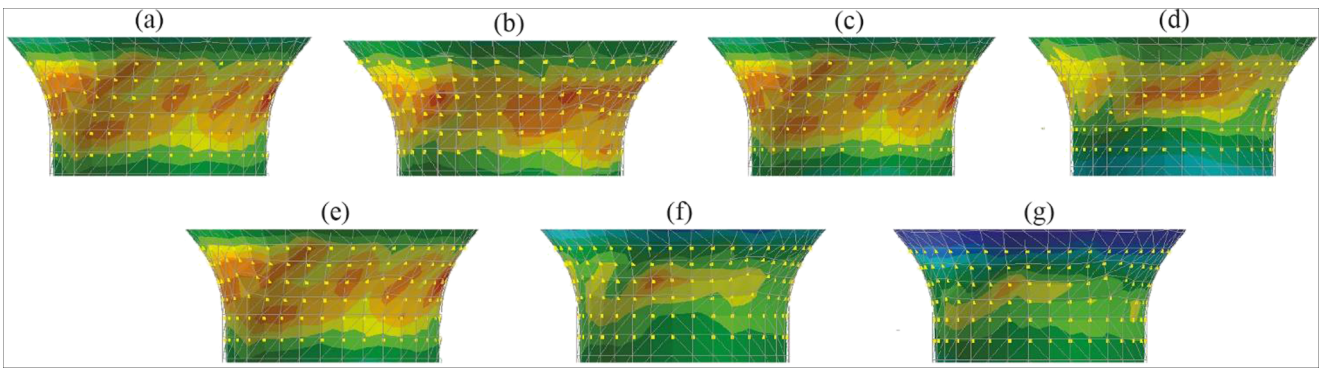

Fig. 10 HTI contours generated in the sensitivity study: **a** 1500 °C pouring temperature, **b** 1400 °C pouring temperature, **c** 0.1 s filling time, **d** 0.5 s filling time, **e** inverse modeling predicted interfacial heat transfer coefficient, **f** constant interfacial heat transfer coefficient, **g** general interfacial heat transfer coefficient for metals

Table 3 Average EPS within the cracking sensitive range during the final stage of solidification

Pin length, in.	EPS plateau		EPS at 0.999 fraction solid, %	EPS at 1.0 fraction solid, %
	Fraction solid	EPS, %		
0.5	0.996	0.73	0.747	0.82
1.0	0.990	0.81	0.825	0.87
1.5, 2.0	0.986	0.87	0.883	0.93

observations of solidification cracking in a Ni-based alloy by Robino et al. [26] and with predicted fraction solid and temperature ranges for NbC and Laves phases in the final stage of solidification of high chromium Ni-based filler metals [27]. However, further research would be required to validate the applicability of these predictions to actual welding scenario.

4.5 Sensitivity study and predicted strain validation

Using the developed FEA model of the CPTT, a series of simulations were performed to evaluate the magnitude of influence of main test variables on the predicted strain accumulation in the crack sensitive region. An initial sensitivity study was focused on the effects of the pouring temperature, mold filling time, and interfacial heat transfer coefficient on the average HTI value within the cracking sensitive region. The results of this study are summarized in Table 4 and Fig. 10.

The sensitivity study showed that the pouring (casting) temperature had insignificant influence on the predicted HTI value. Reduction of the pouring temperature with 100 °C resulted in 0.3% HTI reduction (Table 4 and Fig. 10 (a) and (b)). The pouring temperature in the CPTT is controlled through pyrometer connected within the control loop of the induction power supply and is typically set at 150 °C above the liquidus temperature of the tested alloy. Therefore, pouring temperature variations within a range of 100 °C would not significantly affect the strain accumulation in the cast pin cracking sensitive area.

Extending the mold filling time from 0.1 to 0.5 s reduced the predicted HTI with 7% (Table 4 and Fig. 10 (c) and (d)). The mold filling time of 0.1 s was estimated based on temperature measurements within a cast pin mold instrumented with thermocouples at the pin foot, neck, and half length. The mold filling time would depend on the alloy specific thermophysical properties in liquid state. Based on the result of this study, it is recommended to determine that the mold filling time for tested alloys using thermocouple measurements within the cast pin mold.

Out of the studied parameters, the temperature dependence of the interfacial heat transfer coefficient had the strongest effect on the local strain accumulation. Using a constant value and a generic temperature dependence for metals resulted in deviations of the predicted HTI of 12% and 25.5% correspondingly (Table 4 and Fig. 10 (e), (f), and (g)). Therefore, development of reliable temperature dependences of the interfacial heat transfer coefficient is essential for the accurate predictions of local strain accumulation in the CPTT. Such dependences for tested alloys can be generated using the inverse modeling tool of ProCast™ and thermal histories measured within the CPTT mold.

Validation of the predicted total longitudinal shrinkage in a non-restrained mold was performed to demonstrate the effect of the coefficient of thermal expansion on the prediction accuracy. A 2.0-in. long mold in Alloy C63000 without restraining foot was used in the experimental validation (Fig. 11 (a)). Five pins of Alloy 52M were cast in this mold using the CPTT procedure described in Section 2 and the total longitudinal shrinkage in the five pins was measured. CPTT modeling simulations for the non-restrained mold were conducted using the initial and boundary conditions, and material properties specified in Section 3, including a predicted

Table 4 Sensitivity study parameters and HTI predicted values

Test parameter	Parameter values	Predicted HTI	Effect, %
Pouring temperature, °C	1500*	0.01459	–
	1400	0.01463	0.3
Mold filling time, s	0.1*	0.01459	–
	0.5	0.01355	7.2
Interfacial heat transfer coefficient, W/m^{2}K	Inverse model prediction*, Fig. 3	0.01459	–
	4000	0.01283	12.1%
	500 (room T), 800 (solidus), 1200 (liquidus and pouring)**	0.01087	25.5%

*Parameters used in the presented modeling simulations; **Generic dependence for metals used in ProCAST™

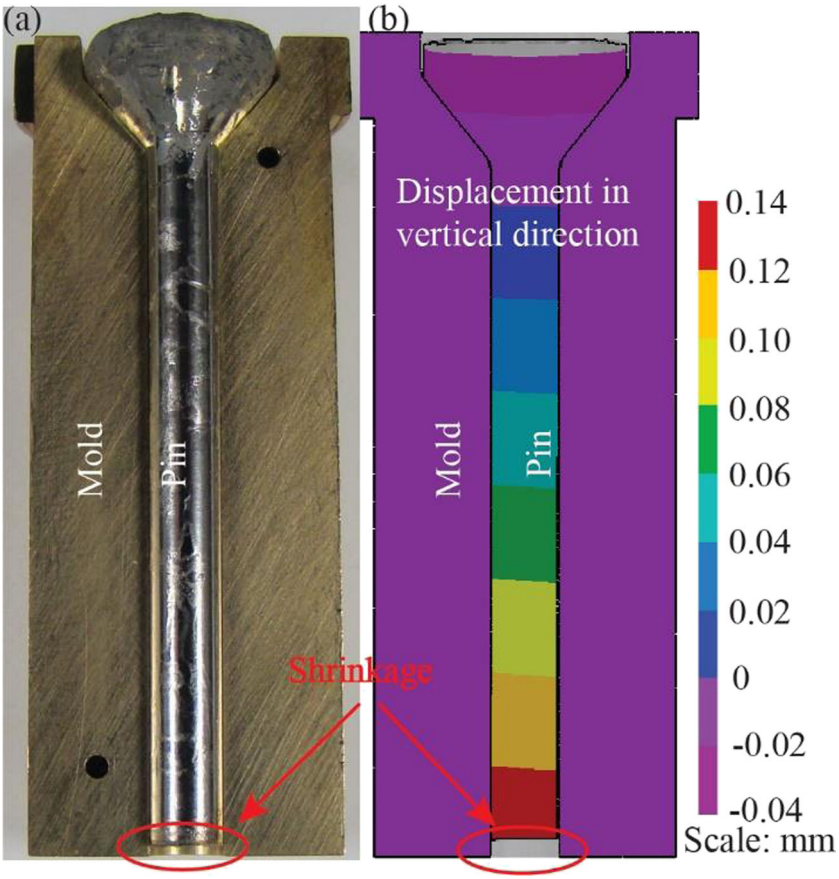

Fig. 11 **a** Cast pin mold without restraining foot used in the strain validation study, **b** FEA modeling prediction of the longitudinal shrinkage in a 2.0-in. long cast pin

temperature dependence of the thermal expansion coefficient. The FEA model of a cast pin within the non-restrained mold is shown in Fig. 11 (b). The predicted longitudinal shrinkage was 1.2 mm, showing a 30% deviation from the 0.9 mm average shrinkage in the five CPTT experiments. Therefore, utilizing an accurate temperature dependence of the coefficient of thermal expansion is essential for the prediction accuracy of the developed CPTT computational model.

5 Summary and conclusions

This study demonstrated that computational modeling of weldability tests can be used as an approach for quantification of material-specific properties related to cracking susceptibility in engineering alloys. FEA model of the cast pin tear test was developed and used in simulations, paralleled with experimentation, to quantify the critical strain for solidification cracking in Alloy 52M. The main conclusions of this study are listed below:

1. The developed FEA model of the cast pin tear test was validated by comparison to CPTT experiments with Alloy 52M filler metal. FEA simulations with this model accurately predicted:

   a. the sequence of solidification and strain accumulation in the cast pin
   b. the cracking sensitive region, including the exact location of crack nucleation and the cracking propagation direction
   c. the relationship of increasing cracking susceptibility, indicated by the hot tearing indicator and the effective plastic strain, with increasing cast pin length

2. The predicted hot tearing indicator and effective plastic strain dependences on the pin length correlated well with observed variations in the CPTT percentage circumferential cracking:

   a. both parameters increased rapidly within the pin length range of crack initiation, which correlated with experimentally observed low variations in circumferential cracking
   b. in the range between 50% and 100% circumferential cracking, the dependence on pin length in both parameters gradually leveled, reflecting wider variations in experimental results

3. Critical strain values for solidification cracking in CPTT of Alloy 52M filler metal were predicted as follows:
   a. critical strain range for crack nucleation between 0.75% and 0.83%, corresponding to minimum pin length with consistent crack initiation of 1.0 in. and predicted fraction solid above 0.98
   b. critical strain for consistent 100% circumferential cracking of 0.88%, corresponding to pin length of 2.0 in.
   c. the above listed predictions were in a reasonable agreement with published data
4. Sensitivity evaluations indicated that the temperature dependences of the interfacial heat transfer and thermal expansion coefficients, along with the mold filling time, had significant effect on the prediction accuracy. Experimental determination is recommended for key material properties and process parameters used with the FEA model of the CPTT.
5. The developed FEA model can be used for quantification of test parameters that are critical for the sensitivity, accuracy, and reproducibility of the CPTT, and for further optimization of testing procedures.
6. Predictions of the critical strain for solidification cracking in the CPTT can be used for reference in the design of welded components and development of welding procedures. However, additional research is needed to correlate predictions of the developed FEA model to actual welding conditions.

Acknowledgements This research was performed at the Welding Engineering Laboratory of The Ohio State University and was supported by Areva, AZZ WSI, Babcock & Wilcox Canada, Böhler Welding Group, the Electric Power Research Institute, and ESI Group North America. The authors acknowledge the technical support of Mr. Samuel Scott of ESI Group North America.

Publisher's note Springer Nature remains neutral with regard to jurisdictional claims in published maps and institutional affiliations.

References

1. Tomota Y, Daikuhara S, Nagayama S, Sugawara M, Ozawa N, Adachi Y, Harjo S, Hattori S (2014) Stress corrosion cracking behavior at Inconel and low alloy steel weld interfaces. Metall Mater Trans A 45(13):6103–6117
2. McCracken SL, Smith RE (2011) Behavior and hot cracking susceptibility of filler metal 52M (ERNiCrFe-7A) overlays on cast austenitic stainless steel base materials. Hot Crack. Phenom. Welds III, p 333–352
3. DuPont JN, Robino CV, Marder AR (1998) Modeling solute redistribution and microstructural development in fusion welds of Nb-bearing superalloys. Acta Mater 46(13):4781–4790
4. DuPont JN, Marder AR, Notis MR, Robino CV (1998) Solidification of Nb-bearing superalloys: part II. Pseudoternary solidification surfaces. Metall Mater Trans A 29(11):2797–2806
5. Engel R, Heldt J, Krause C (2013) Design and Analysis of a Full Structural Weld Overlay for a Feedwater Nozzle-to-Safe End Dissimilar Metal Butt Weld. Transactions, SMiRT-22, p Division VI
6. Mccracken SL, Tatman JK (2012) Influence of Austenitic Stainless Steel Base Metals on Hot Cracking Susceptibility of High Chromium Nickel-base Filler Metals. Proceedings of the 2012 ASME Pressure Vessels & Piping Division Conference, p PVP2012–78614 (1)–(11)
7. Ramirez J (2011) Understanding stress corrosion cracking of welds in nuclear reactors. Weld J 7:38–42
8. Cofie NG, et al (2008) Effectiveness of Stainless Steel Buffer Layer to Address Hot Cracking During Weld Overlay Repair of Dissimilar Metal Alloy 82/182 Welds with Stainless Steel Piping. Proceedings of 2008 ASME Pressure Vessels and Piping Division Conference, p PVP2008–61411 (1)–(10)
9. Hull FC (1959) Cast-pin tear test for susceptibility to hot cracking. Weld J 38:176–181
10. McCracken SL, et al (2010) Hot Cracking Study of High Chromium Nickel-Base Weld Filler Metal 52MSS (ERNiCrFe-13) for Nuclear Applications. Pressure Vessels & Piping PVP10, Paper PVP2010–25787, ASME, 2010(49255), p 879–889
11. Alexandrov BT, Lippold JC (2013) Use of the cast pin tear test to study solidification cracking. Weld World 57(5):635–648
12. Luskin TC (2013) Investigation of weldability in high-Cr Ni-base filler metals. The Ohio State Univeristy Thesis
13. Alexandrov BT, Lippold JC, Nissley NE (2008) Evaluation of weld solidification cracking in Ni-base superalloys using the cast pin tear test. In: Hot cracking phenomena in welds II, T. Böllinghaus, et al. Springer Berlin Heidelberg, Berlin, pp 193–213
14. Alexandrov B et al (2013) Susceptibility to solidification cracking in high chromium nickel-base filler metals for nuclear power applications, Trends in Welding Research IX, ASM International, pp 614–622
15. Dong H, Gao H, Wu L (2003) Numerical simulation of heat transfer and fluid flow in a double-sided gas-tungsten arc welding process. Proc Inst Mech Eng B J Eng Manuf 217(1):87–97
16. Niel A, Bordreuil C, Deschaux-Beaume F, Fras G (2013) Modelling hot cracking in 6061 aluminium alloy weld metal with microstructure based criterion. Sci Technol Weld Join 18(2):154–160
17. Wei YH, Dong ZB, Liu RP, Dong ZJ (2005) Three-dimensional numerical simulation of weld solidification cracking. Model Simul Mater Sci Eng 13(3):437–454
18. Dong ZB, Wei YH (2006) Three dimensional modeling weld solidification cracks in multipass welding. Theor Appl Fract Mech 46(2):156–165
19. Coniglio N, Cross CE (2013) Initiation and growth mechanisms for weld solidification cracking. Int Mater Rev 58(7):375–397
20. Safari AR, Forouzan MR, Shamanian M (2012) Hot cracking in stainless steel 310s, numerical study and experimental verification. Comput Mater Sci 63:182–190
21. Eskin DG, Suyitno, Katgerman L (2004) Mechanical properties in the semi-solid state and hot tearing of aluminium alloys. Prog Mater Sci 49(5):629–711
22. Zhu JZ, Guo J, Samonds MT (2011) Numerical modeling of hot tearing formation in metal casting and its validations. Int J Numer Methods Eng 87(1–5):289–308

23. Wang Z, Huang Y, Srinivasan A, Liu Z, Beckmann F, Kainer KU, Hort N (2014) Experimental and numerical analysis of hot tearing susceptibility for Mg-Y alloys. J Mater Sci 49(1):353–362
24. Luskin TC et al (2012) Preliminary Finite Element Analysis and Optimization of the Cast Pin Tear Test. in Numerical Analysis of Weldability X. Technische Universität Graz, Graz
25. Przybylowicz E et al (2016) Weldability evaluation of high chromium, Ni-base filler metals using the cast pin tear test. In: Boellinghaus T, Lippold JC, Cross CE (eds) Cracking phenomena in welds IV. Springer International Publishing, Cham, pp 269–288
26. Robino CV (2016) Engineering approximations in welding: bridging the gap between speculation and simulation. Weld J 95:1s–16s
27. Przybylowicz E (2014) Weldability evaluation of high-Cr Ni-base filler metals using the cast pin tear test. The Ohio State University, Columbus